

**Controls on fault-hosted fluid flow; Preliminary results from the Coso
Geothermal Field, CA**

Nicholas C. Davatzes*
Stephen H. Hickman

U.S. Geologic Survey 345 Middlefield Road, MS 977
Menlo Park, CA 94025

Paper 144

Key words: Cap rock, permeability, fault, fracture, clay, Coso

* Corresponding author:
Tel: 650-329-4024
e-mail: ndavatzes@usgs.gov

Abstract

Initial examination of fault rock mineralogy and associated deformation mechanisms in the Coso Geothermal Field distinguishes three fault types: (1) Fault rocks dominated by kaolinite and quartz with associated dissolution and dilatant brittle fracturing; (2) Fault rock dominated by foliated chlorite-smectite, which accommodates slip through ductile shearing and folding; and (3) Fault rock consisting of cataclastic gouge abraded from the host rock, which exhibits crack-seal textures resulting from repetitive brittle failure, dilation, and precipitation of quartz or calcite. These different fault zones are respectively associated with the upper boiling zone of the reservoir, a conductively heated “caprock” at moderate to shallow depth associated with low permeability, and a deeper convectively heated region associated with enhanced permeability. We suggest that chemical alteration of otherwise low-porosity crystalline rocks can produce a change in deformation mechanism that in turn controls the distribution of permeability in the actively deforming geothermal system.

Introduction

In crystalline rock, faults and fractures provide the primary source of permeability. Yet the active precipitation of minerals and chemical alteration in many hydrothermal systems implies that fractures conducting fluids in the subsurface will often seal and permeability will be lost. In contrast, recurrent brittle fracture and frictional failure in low porosity crystalline rocks produce dilation owing to surface roughness along the fracture walls (Brown, 1987) and the formation of breccias and microcracks during fault slip (Lockner and Beeler, 2002). Faults and fractures sealed by the precipitation of common vein-filling minerals such as quartz or calcite retain this brittle (dilatant) behavior, as demonstrated by crack-seal textures in layered veins or the brecciation of fault cements. These processes lead to periodic permeability enhancement associated with reactivation of optimally oriented and critically stressed fractures, which has been shown to be an important mechanism in maintaining high reservoir permeability in some geothermal systems (Barton *et al.*, 1998).

Alternatively, dissolution of crystalline rock by hydrothermal fluids reduces the strength of grain contacts and increases porosity in fracture walls (Boitnott, 2002). Chemical alteration can also produce increasing proportions of clays and other phyllosilicates, which promote ductile behavior and reduce frictional strength (Lockner and Beeler, 2002) while also reducing fault permeability (Crawford *et al.*, 2002). The potential result of these processes is increased ductility of fault rocks that minimizes dilation accompanying slip and prevents regeneration of permeability.

Geothermal systems are commonly recognized to consist of a clay-rich caprock, situated above a permeable reservoir zone, and at greater depth, a plastically deforming zone. In this contribution we explore how mineralogical and petrophysical properties associated with these zones in the Coso Geothermal Field control mechanisms that accommodate deformation and consequently determine the permeability of newly formed or reactivated fractures. We find that the permeability structure of the Coso Field is likely generated and maintained through a feedback between recurrent fracture slip and fluid flow on one hand and mineral precipitation and chemical alteration on the other.

Geological Setting

The Coso Geothermal Field is rooted in dominantly granitoid rocks overlain by rhyolites and basalts. It is located immediately east of the Sierra Nevada at the transition from dextral strike-slip tectonics, characteristic of the San Andreas Fault system, to east-west extension along Basin and Range style normal faults (Figure 1a). A shallow silica-rich partial melt topping out at 4-5 km depth provides both the source for recently extruded volcanic materials and high modern heat flow (Unruh and Hauksson, 2003; Manley and Bacon, 2001). Alteration in the Coso Geothermal Field varies with temperature and depth (Lutz *et al.*, 1996; Kovac *et al.*, 2005) and defines a caprock of clay-dominated alteration. These clay-bearing intervals coincide with high geothermal gradients and are consistent with conductive heat transfer and low permeability situated above the exploited geothermal reservoir. Development of that geothermal reservoir has provided an electric power generating capacity in excess of 240 MW (Adams *et al.*, 2000).

Methods

We use several lines of evidence to infer the mechanisms by which faults at Coso form and slip and how this, in turn, controls the permeability structure of the Coso Geothermal Field. Surface outcrops, core, and image logs constrain the geometry, mineralogy, and textures of the structures in fault zones. These data are used to infer the mechanisms of deformation and fault-slip behavior (Davatzes *et al.*, 2005). Modern and paleo-fluid flow within the geothermal field are inferred from the distribution of fluid flow at the surface, temperature profiles, mud loss during drilling, and the distribution of seismicity. Fluid flow data and deformation data are cross-correlated to establish the relationship of fault zones to fluid flow.

Fault zones structure and deformation mechanisms

We have distinguished three distinct types of fault zones within the Coso Geothermal Field: (1) Fault zones containing intense alteration, resulting in disaggregation and subsequent replacement of most rock-forming minerals with kaolinite; (2) Fault zones associated with breccia, high fracture density, locally large fracture aperture, and fractures healed by the precipitation of calcite; and (3) Fault zones with a core dominated by chlorite and smectite fault rocks surrounded by highly fractured host rock and rare calcite veins. In the following sections, we describe these fault zones using representative examples (locations shown in Figure 1c), interpret the mechanisms of deformation, and explore their implications for the physical behavior and development of the fault zone.

(1) Pervasively altered fault rocks rich in kaolinite and silica

An example of an altered kaolinite-rich fault zone is exposed by excavation of the mercury mine at the Nicol Prospect (Figure 2a). The fault core (the part of the fault that accommodates most of the deformation and shear strain) is comprised of kaolinite-rich fault gouge (Figure 2a, b) and isolated breccia clasts. The gouge zone contains a through-going striated slip surface (Figure 2c) and subsidiary shorter slip surfaces. The through-going slip surfaces are coated by and incorporate microspheres of amorphous silica (Figure 2d). The major rock-forming minerals such as feldspar, hornblende, and biotite have been leached out of the breccia clasts, increasing the porosity, and are partly replaced with alteration phases such as kaolinite (Figure 2e). The core of the fault is surrounded by highly fractured rocks comprising a damage zone with minor mineralization and small slickensided faults exhibiting several

centimeters of down-dip (normal faulting) slip. Intense alteration is primarily confined to the fault core and becomes less intense with greater distance from the slip surface. This distribution of alteration is consistent with fluid flow primarily focused along the slip surface and bleeding out into the surrounding gouge and fractured damage zone.

(2) *Brecciated, dilatant, calcite rich fault zones*

Different fault zone mineralogy and structure are evident in the damage zone of the Coso Wash normal fault (Figure 3a) exposed NNE of the Coso Wash Hot Springs. At that location, the damage zone is comprised of a series of small faults and fractures that mirror the local orientation of the modern fault scarp. Many of these fractures contain fibrous veins more than 10 cm thick (Figure 3b) consistent with deposition into void space. Dilatant (tensile) fractures also occur in association with sheared fractures (Figure 3c). In general, the tensile fractures intersect the sheared fracture at an angle approximately between 50° and 75° and are asymmetrically distributed about it. This geometry and age relationship is consistent with the formation of splay fractures that propagate in response to tensile stresses concentrated at the tip or at asperities of a slipping shear fracture (Davatzes and Aydin, 2003). Splay fractures are densest in extensional steps between two overlapping, *en echelon* sheared fractures (Figure 3c) where they define fracture-bounded rhombs of rock. Shearing of fractures healed by precipitation (Figure 3d) is associated with the rotation of the fracture-bounded volumes and the formation of breccia, indicating that fracture porosity is regenerated following healing.

(3) *Chlorite-smectite rich fault zones*

The third fault zone type is distinguished by a fault core dominantly composed of chlorite and smectite (Figure 4a). Multiple, linking slip surfaces are distributed across the fault core and anastomose around more intact blocks of the host rock (as shown in Figure 4b). Slip surfaces are polished and coated by chlorite and smectite. Within the shear zone the chlorite shows foliation subparallel to the fault strike and dip. Porosity is relatively low in the fault rock, and pores appear to be isolated. The textural relationship of the fault rock to the breccia blocks and margins of the fault core indicates relatively ductile deformation by folding of chlorite and smectite foliation and extrusion of clay into void space. Adjacent to the fault core, the country rock is highly fractured. Breccia and brittle fractures in the damage zone are well-connected and dense, but do not cross the fault core.

Evidence for the fluid flow behavior of faults

Fluid flow along faults in the Coso Geothermal Field is indicated by the preferred distribution of surface alteration, fumaroles, and steaming ground along faults and at some fault intersections (Figure 1c). The most predominant active surface flow is associated with NNE trending normal faults that are well oriented for slip in the modern stress state (Figure 1c) and show geomorphic evidence for slip, including offset alluvial fans. Subsurface fluid flow along faults is indicated by perturbations in borehole temperature logs (see discussion in Barton et al, 1998) and mud losses that coincide with faults visible in image logs (see example from well 58A-10 in Figure 5). In addition, near-isothermal temperature gradients, such as seen in well 58A-10 over the depth interval labeled zone 2 (Figure 5), indicate convective fluid flow that requires high permeability along a network of fractures.

It is more difficult to determine where faults act as barriers to fluid flow, although this can be inferred from borehole temperature logs in addition to the distribution of seismicity. The repeat temperature logs from well 58A-10 (Figure 5) distinguish two zones of high temperature gradient labeled zones 1 and 3. These high temperature gradients suggest conductive heat transfer and low permeability, despite fracture densities and orientations similar to zone 2, where convection dominates (Davatzes and Hickman, 2005). Another important aspect of zone 2 is the presence of very small but abrupt changes in geothermal gradient across faults (labeled as sub-zones A-E in Figure 5). These small-scale transitions in gradient are consistent with these faults acting as limited, or transient, barriers to fluid flow.

In addition, locally high rates of seismicity within the actively produced Coso Geothermal Field and the spatial association of this seismicity with boreholes suggest that most micro-earthquakes are probably related to fluid pressure variations induced by fluid production or injection (Feng and Lees, 1998). However, sharply defined margins to this otherwise diffuse seismicity coincide with faults visible at the surface (Figure 1b). These sharply defined terminations of seismicity indicate that these faults act as barriers to fluid flow, limiting the spatial extent of fluid pressure variation and effectively compartmentalizing the Coso Geothermal Field.

In most locations, faults display indications of both focused fluid flow and barrier behavior. One example is the fault seen at 6900 ft in well 58A-10 (Figure 5), which was associated with significant mud losses while drilling and persistent negative temperature gradients. This fault also separates adjacent sub-zones of distinct temperature gradient. Similarly, the Coso Wash normal fault system (Figure 1c) hosts fumaroles but also defines the margins of earthquake clusters (Figure 1b). In both cases fluid flow across the fault appears to be inhibited, whereas fluid flow along the fault is enhanced.

Conceptual model of fluid flow and fault mechanics in the Coso Geothermal System

The distribution of active fumaroles and steaming ground at the surface (Figure 1c) indicate that fluid flow is primarily associated with active fault segments trending NNE and at intersections between fault segments. However, not all of the faults (or fault segments) seen at Coso appear to be permeable. For example, the temperature profiles (Figure 5) and geologic well log from well 58A-10 suggest that the conductive zone of low fluid flow (zone 1) is associated with abundant clay mineralization, in contrast to the convecting zone (zone 2) which is associated with calcite precipitation and little alteration.

Furthermore, the mineralogy and texture of the different fault zones identified at Coso (Figures 2, 3, and 4) indicate the role of different deformation mechanisms and structural/geochemical history. For example, faults healed by the precipitation of calcite and related minerals continue to undergo brittle dilation when reactivated and thus regenerate permeability (Figure 3). In contrast, the introduction of chlorite and other sheet silicates such as smectite appear to promote ductility and thereby minimize dilatancy of the fault rock during shear (Figure 4). In the following sections we discuss the relationship of the deformation mechanisms that control fluid flow to the deformation environments defined by the shallow

ground water system, clay-rich caprock, reservoir interval, and partial melt that define the Coso Geothermal System. This discussion is indexed to the four zones shown in Figure 6b.

Zone 1. Shallow groundwater flow: In the shallowest zone, groundwater flow circulates through a network of diffusely distributed fractures associated with active faulting and dilatant failure facilitated by low confining stress. Rising geothermal fluids or boiling in areas of high heat flow and slow recharge exsolve gases that can mix with shallow groundwater, potentially lowering the pH and promoting mineral dissolution (Facca and Tonani, 1967). Dissolution of major rock-forming minerals such as feldspar, plagioclase, hornblende, pyroxene and biotite should initially increase fault zone permeability. This overall gradual increase in permeability will be augmented by sudden permeability increases induced by dilatancy accompanying episodic fault slip (spikes in Figure 6d).

Zone 2. Caprock: The caprock is characterized by conductive heat flow and minimal circulation of fluid. Initial fault formation and slip is the result of brittle-dilatant failure. However, continued slip and fluid flow leads to the formation of smectite phases and chlorite that inhibit dilation accompanying slip. Alteration is greatest in the fault core and decreases into the host rock. As a result, any damage outside the fault core in unaltered rock remains dilatant. Consequently, fault-parallel permeability increases as cross-fault permeability decreases. The net result is the progressive development of faults with low cross-fault permeability and enhanced fault-parallel permeability. Although permeability might increase in the fault damage zones, the intersection of non-parallel (e.g., conjugate) fault cores truncates the damage zone, leading to a caprock with low overall permeability. Over the lifetime of the geothermal system, continued alteration should further isolate and reduce the size of zones of dilatant failure that generate fracture permeability.

The vertical permeability seal provided by this “clay-rich cap” could be breached by the development of (1) new fault networks or (2) localized dilation related to fault geometry. New fault networks form when there is a sudden change in tectonic stress that is unfavorable for reactivation of an established fault network. Because alteration is primarily localized along the older fault networks, new faults will principally propagate through nearly unaltered rock that favors brittle failure. Owing to the low frictional strength of most clays (Lockner and Beeler, 2002), large rotations of the stress state are required to create new faults in a clay-rich cap, suggesting that breaching of the cap rock by new fault networks will be more difficult. Also, mechanical interaction of fault segments at extensional steps or intersections can locally produce more tensile mean stress that promotes dilatant failure (Davatzes *et al.*, 2005). This mechanism could produce a pathway for fluids to migrate from reservoir depths to the surface along parts of faults—essentially breaching the cap rock.

Zone 3. Reservoir zone: The reservoir zone is dominated by brittle fracture, brecciation, and cataclasis. Healing primarily occurs by the precipitation of calcite or silica (potentially promoted by convection). In general, the near absence of clays and other phyllosilicates in the reservoir zone prevents the formation of a persistently low-permeability fault core. Thus, across-fault as well as along-fault permeability will be regenerated by periodic fault slip (Figure 6d). In detail, reduced grain size in the fault core due to cataclasis increases the area of fresh mineral surfaces and the rate of chemical reactions and precipitation on those surfaces. This suggests that the core of reservoir faults will heal faster than the damage zone during the inter-seismic period and thus

produce transient across-fault barriers or low-permeability zones (Byerlee, 1993). Consequently, convection can be temporarily confined within isolated damage zones resulting in small steps in temperature gradient (shown diagrammatically in Figure 6b), even though these transient seals will be periodically ruptured so that the permeability within the reservoir remains generally high.

4. Crystal-plastic deformation below the brittle-ductile transition: As temperature increases with depth and proximity to the heat source, crystal plastic deformation becomes the dominant means of accommodating strain. Large earthquakes can locally extend the depth of micro-seismicity (as indicated by the jagged top of the brittle-ductile transition in Figure 1b) by locally increasing the strain rate. However, the permeability of fault and country rock in this zone is expected to be quite low.

Conclusions

The feedback between fracture slip, the generation of permeability, fluid flow and alteration suggests that fracture permeability will evolve concurrently with the geothermal system. Initial fracture development in un-altered crystalline rocks will enhance permeability and allow the circulation of fluids, the transfer of heat, and initiate chemical alteration. Chemical alteration will eventually lead to the breakdown of rock forming minerals and alteration to clays within appropriate temperature and pressure conditions. The presence of clay in the cap rock mitigates the ability of fracture slip to generate permeability and consequently isolates a deeper geothermal reservoir from the surface. In contrast, in reservoir rocks permeability is maintained in fracture systems of calcite- or silica-dominated fracture sealing through dilatancy accompanying episodic slip despite exposure to the same stress state and deformation conditions as in the cap rock.

Acknowledgments

Much of the data analyzed was made available through the Navy Geothermal Program Office. John Solum and Joe Moore provided valuable feedback. Steve Bjornstad, Patrick Muffler and Colin Williams provided critical reviews of the science and text. David Blackwell reviewed the manuscript for the Geothermal Resources Council. Funding was provided by the U.S. Geological Survey Mendenhall Fellowship.

References

- Adams, M.C., Moore, J.N., Bjornstad, S., and Norman, D.I. 2000. Geologic history of the Coso Geothermal Field. Proceedings World Geothermal Congress 2000, Kyushu – Tohoku, Japan, May 28 – June 10, 2000. p. 2463-2469.
- Barton, C., Hickman, S., Morin, R., Zoback, M.D., and Benoit, R., 1998, Reservoir-scale fracture permeability in the Dixie Valley, Nevada, geothermal field, in *Rock Mechanics in Petroleum Engineering*, vol. 2, R. M. Holt et al. (eds.), Society of Petroleum Engineers, Richardson, TX., p. 315-322.
- Boitnott, G.N. 2002. Core analysis for the development and constraint of physical models of geothermal reservoirs. *Geothermal Research Council Transactions* 26, 387-392.

- Brown, S.R. 1987. Fluid flow through rock joints: Effects of surface roughness. *J. Geophys. Res.* 99, p. 9373-9390.
- Byerlee, J.D. 1993. A model for episodic flow of high pressure water in fault zones before earthquakes. *Geology*, 21, p. 303-306.
- Crawford, B.R., Myers, R.D., Woronow, A., Faulkner, D.R., and Rutter, E.H. 2002. Porosity-permeability relationships in clay-bearing fault gouge. *SPE/IRSM 78214*, p. 1-13.
- Davatzes, N.C. and Hickman, S. 2005. Comparison of acoustic and electrical image logs from the Coso Geothermal Field, CA. *Proceedings, Thirtieth Workshop on Geothermal Reservoir Engineering*, Stanford University, January 31- February 2, 2005. SGP-TR-176, p. 1-11.
- Davatzes, N.C. and Aydin, A. 2003. The formation of conjugate normal fault systems in folded sandstone by sequential jointing and shearing, Waterpocket monocline, Utah. *Journal of Geophysical Research* 108(B10), p. 2478-2493.
- Davatzes, N.C., Eichhubl, P., and Aydin, A. 2005. Structural evolution of fault zones in sandstone by multiple deformation mechanisms; Moab Fault, southeast Utah. *Geological Society of America Bulletin*, vol.117, no.1-2, p.135-148
- Facca, G. and Tonani, F. 1967. The self-sealing geothermal field. *Bulletin of Volcanology*, 30, p. 271-273.
- Feng, Q. and Lees, J.M. 1998. Microseismicity, stress, and fracture in the Coso geothermal field, California. *Tectonophysics*, 289, p. 221-238.
- Geomechanics International. 2003. Fracture permeability and in situ stress in the eastern extension of the Coso Geothermal Reservoir; Kinematic and dynamic studies of the Coso Geothermal and surrounding area. Report prepared for the Navy Geothermal Program Office. Report number N68936-01-R-0095. 75 p.
- Hulen, J. B. 1978. *Geology and alteration of the Coso geothermal area, Inyo County, California*. U. S. Department of Energy: Geothermal Energy.
- Kovac, K.M. Moore, J.N., and Lutz, S.J. 2005. Geologic framework of the East Flank, Coso Geothermal Field: Implications for EGS development. *Thirtieth Workshop on Geothermal Reservoir Engineering*, Stanford University, Stanford, California, January 31-February 2, 2005, SGP-TR-176, 7 p.
- Lockner, D.A. and Beeler, N.M. 2002. Rock failure and earthquakes. *International Handbook of Earthquake and Engineering seismology*, 81A, p. 505-537.
- Lutz, S.J., Moore, J.N., Copp, J.F. 1996. Integrated mineralogical and fluid inclusion study of the Coso Geothermal System, California. *Proceedings, 21st Workshop on Geothermal Reservoir Engineering*, Stanford University, Stanford, California, p. 187-194.
- Manley, C.R. and Bacon, C.R. 2000. Rhyolite thermobarometry and the shallowing of the magma reservoir, Coso Volcanic Field, California. *J. Petrol.* 41, p. 149-174.
- Moore, J., Norman, D., and Adams, M. 2004. Thermal and chemical history of the Eastern Coso Geothermal Field. Report to the Navy Geothermal Program Office. Report N68936-01-0095. 71 p.
- Sheridan, J. and Kovac, K.M., Rose, P. E., Barton, C. A., McCulloch, J., Berard, B., Moore, J. N., Petty, S. & Spielman, P. 2003. In situ stress, fracture and fluid flow analysis-East Flank of the Coso Geothermal Field. *Twenty-eighth Workshop on Geothermal Reservoir Engineering*, Stanford University, Stanford, California, January 27-29, SGP-TR-173, 16 p.
- Unruh, J. R. and Hauksson, E. 2003. Seismotectonics of an Evolving Intra-Continental Plate Boundary, East-Central California. *Geothermal Program Office Technical Symposium 8*, University of California, Davis, CA.

Whitmarsh, R.C. 1998. Structural development of the Coso Range and adjacent areas of eastern California [Ph.D. thesis]: Lawrence, Kansas, University of Kansas.

Figure Captions

Figure 1: (a) Location map of the Coso Geothermal Field. (b) Cross section of seismicity from 1993 to 2003 at the Coso Geothermal Field recorded by the local seismometer network operated by the Navy Geothermal Program Office. We infer that the brittle-ductile transition roughly coincides with the abrupt decrease in earthquake occurrence. (c) Tectonic map of the east flank of the Coso Geothermal field. Minimum horizontal stress orientations inferred from borehole image logs were compiled from Geomechanics International (2003), Sheridan *et al.* (2003), and Davatzes and Hickman (2005). Location of alteration, fumaroles, and steaming ground is based on new mapping and results from Hulen (1978) and Whitmarsh (1998).

Figure 2: (a) Map of altered kaolinite-rich fault zone (location Figure 1c) distinguishing zones of different deformation and alteration intensity. Scanning Electron Microscope images of (b) foliated kaolinite-rich fault gouge, (c) striated fault slip surface, (d) microspheres and rod-like structures of amorphous silica, and (e) altered breccia clasts.

Figure 3: (a) Geologic map of the Coso Wash fault scarp and zones of massive veins and breccia in granodiorite (location Figure 1c). Detailed photos of damage zone structures including: (b) layered carbonate vein, (c) dilatant fractures (splay fractures) localized between sheared fractures, (d) breccia and associated splay fractures.

Figure 4: (a) Oblique photograph and sketch map of fault zone rich in chlorite (strike/dip = $\sim 303/50^\circ$) (location Figure 1c). (b) Core from a depth of 679 ft with similar structures from well 64-16.

Figure 5: Repeat temperature profiles measured in well 58A-10 located in Coso Wash (location Figure 1c), mud losses while drilling (spikes), stress rotations (Davatzes and Hickman, 2005), and unwrapped borehole televiewer image and caliper log of fault zone at 6900 ft measured depth.

Figure 6: Conceptual model of fluid flow along faults in a geothermal system. The approximate distribution of alteration clay phases follows the work of Lutz *et al.*, (1996), Moore *et al.* (2004), and Kovac *et al.* (2005).

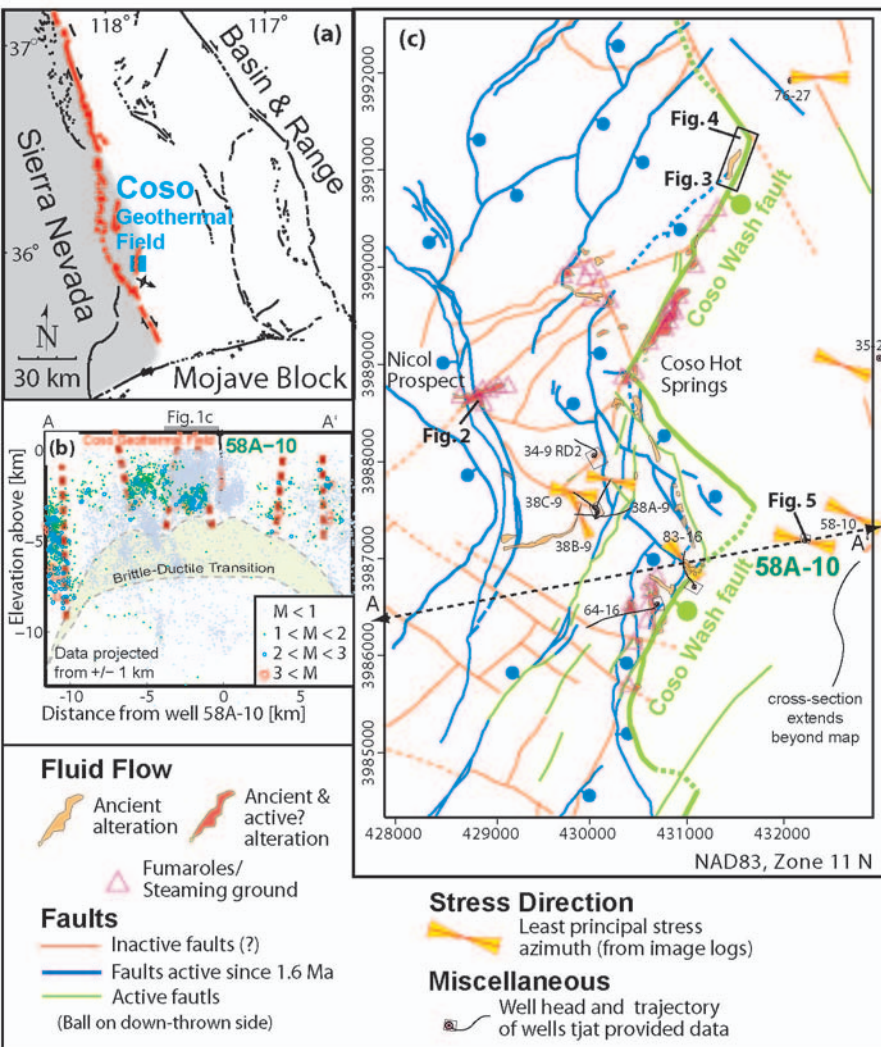


Figure 1

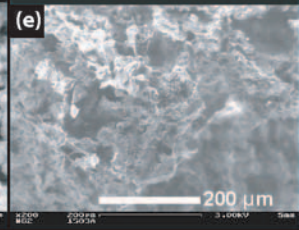
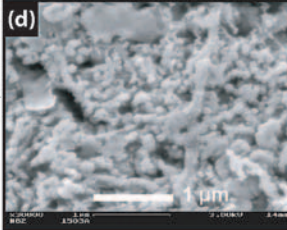
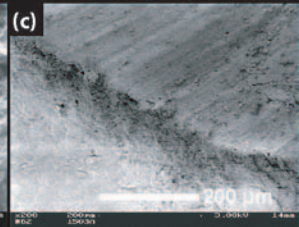
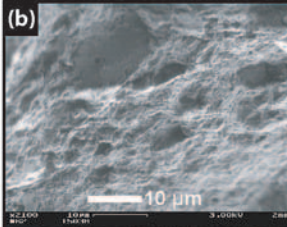
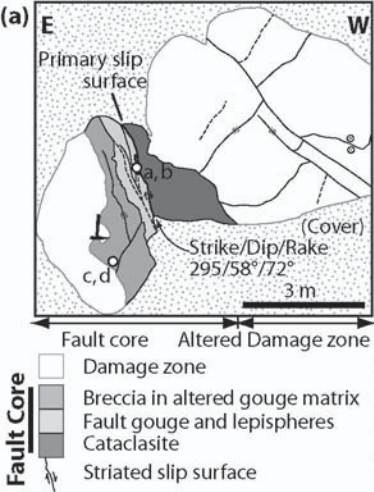


Figure 2

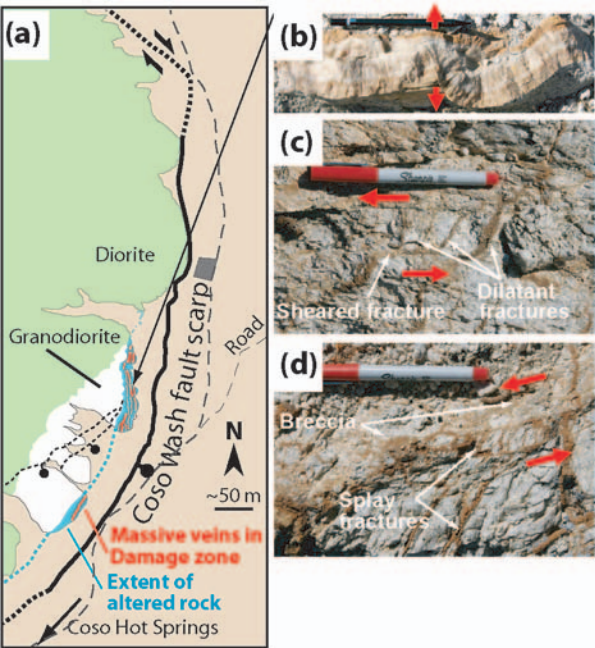


Figure 3

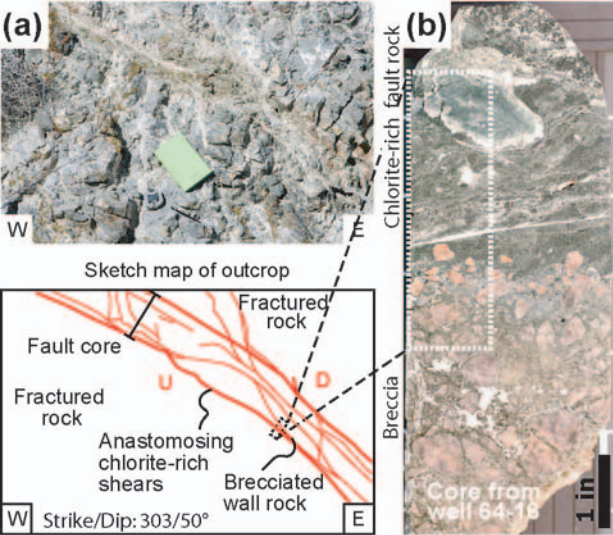


Figure 4

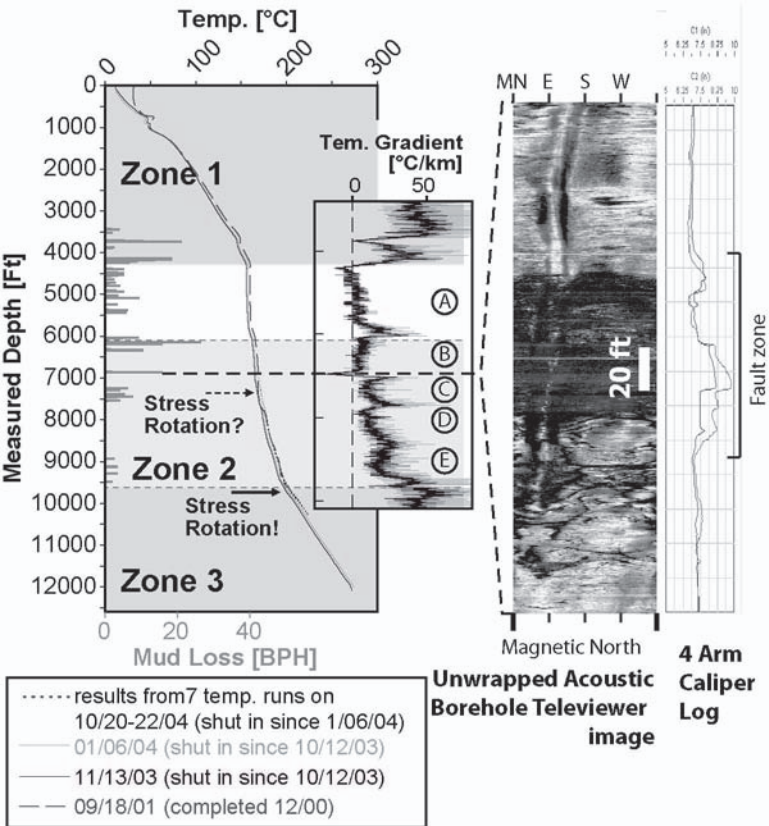


Figure 5

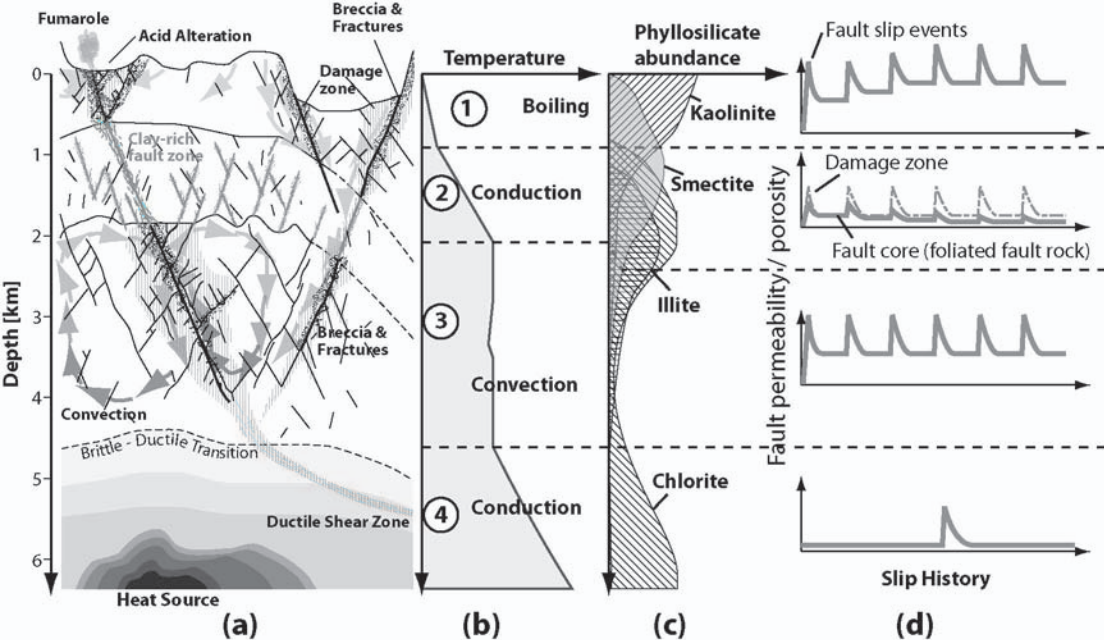


Figure 6